Inorg. Chem. **2005**, *44*, 3441–3448

Synthesis and Structural Characterization of Some Selenoruthenates and Telluroruthenates

Sergey M. Dibrov,[†] Bin Deng,[†] Donald E. Ellis,[‡] and James A. Ibers*,[†]

Department of Chemistry and Department of Physics & Astronomy, Northwestern University, 2145 Sheridan Road, Evanston, Illinois 60208-3113

Received November 18, 2004

The reaction of solid $[RuClCp(PPh_3)_2]$ with $TeSe_3^{2-}$ or Se_n^{2-} in DMF leads to the formation of $[RuCp(PPh_3)(\mu_2\text{-}Se_2)]_2$ (**1**). In the structure of this compound the two bridging Se_2 groups lead to a six-membered Ru_2Se_4 ring in a chair conformation. Attached to each Ru center is a PPh_3 ligand in an equatorial position and a Cp ring in an axial position. The compound is diamagnetic. The compound $[Ru_2Cp_2(\mu_3\text{-}Se_2)(\mu_3\text{-}Se)]_2$ (**2**) is obtained under similar conditions in the presence of air. This structure comprises a centrosymmetric Ru_4Se_6 dimer formed from the two bridging Se groups and the two bridging Se_2 groups. Each Ru center is π-bonded to a Cp ring. The reaction of solid $[RuClCp(PPh_3)_2]$ with a Te_n^{2-} polytelluride solution in DMF leads to the diamagnetic compound $[(RuCp(PPh_3))_2(\mu_2\text{-}(1,4\text{-}\eta\text{:}3,6\text{-}\eta)Te_6)]$ (**3**). Here the Ru centers are bound to a bridging Te_6 chain at the 1, 4, 3, and 6 positions, leading to a bicyclic Ru_2Te_6 ring. Each Ru atom is bound to a Cp ring and a PPh_3 group. This dimer possesses a center of symmetry. The structure of **3** is the first example of a bicyclic complex where fusion occurs along a Te–Te bond. If the same reaction is carried out in DMF/CH_2Cl_2, rather than DMF, then $[(RuCp(PPh_3))_2(\mu_2\text{-}(1,4\text{-}\eta\text{:}3,6\text{-}\eta)Te_6)]\cdot CH_2Cl_2$ (**4**) is obtained. In the solid state it possesses the same Ru_2Te_6 structural unit as does **3**, but the unit lacks a crystallographically imposed center of symmetry. The electronic structures of **3** and **4** have been analyzed with the use of first principles density functional theory. Bond order analysis indicates that the Te–Te bond where fusion occurs has a shared bonding charge of about $^2/_3$ of that found for Te–Te single bonds.

Introduction

Many polychalcogenide anions have been isolated and structurally characterized by single-crystal diffraction methods.[1−13] These anions have been employed in the development of an extensive polychalcogenometalate chemistry.[14−19] A number of different compounds of the type $M(\mu\text{-}Q_n)_2M$ (where Q = S, Se, Te; M = metal) have been synthesized and structurally characterized. The most common of this type are $M(\mu\text{-}Q_2)_2M$ six-membered ring compounds of Co,[20] Ru,[21,22] and Ti,[23] and $M(\mu\text{-}Q_3)_2M$ eight-membered

* To whom correspondence should be addressed. E-mail: ibers@chem.northwestern.edu.
[†] Department of Chemistry.
[‡] Department of Physics & Astronomy.

(1) Brese, N. E.; Randall, C. R.; Ibers, J. A. *Inorg. Chem.* **1988**, *27*, 940−943.
(2) Sheldrick, W. S.; Braunbeck, H. G. *Z. Naturforsch. B: Anorg. Chem. Org. Chem.* **1989**, *44*, 1397−1401.
(3) Fenske, D.; Kräuter, G.; Dehnicke, K. *Angew. Chem., Int. Ed. Engl.* **1990**, *29*, 390−391.
(4) Müller, V.; Dehnicke, K.; Fenske, D.; Baum, G. *Z. Naturforsch. B: Chem. Sci.* **1991**, *46*, 63−67.
(5) Staffel, R.; Müller, U.; Ahle, A.; Dehnicke, K. *Z. Naturforsch. B: Chem. Sci.* **1991**, *46*, 1287−1292.
(6) Krebs, B.; Lührs, E.; Willmer, R.; Ahlers, F.-P. *Z. Anorg. Allg. Chem.* **1991**, *592*, 17−34.
(7) Huang, S.-P.; Dhingra, S.; Kanatzidis, M. G. *Polyhedron* **1992**, *11*, 1869−1875.
(8) Müller, V.; Grebe, C.; Müller, U.; Dehnicke, K. *Z. Anorg. Allg. Chem.* **1993**, *619*, 416−420.
(9) Müller, V.; Ahle, A.; Frenzen, G.; Neumüller, B.; Dehnicke, K.; Fenske, D. *Z. Anorg. Allg. Chem.* **1993**, *619*, 1247−1256.
(10) Smith, D. M.; Ibers, J. A. *Coord. Chem. Rev.* **2000**, *200*−*202*, 187−205.
(11) Björgvinsson, M.; Sawyer, J. F.; Schrobilgen, G. J. *Inorg. Chem.* **1991**, *30*, 4238−4245.
(12) Björgvinsson, M.; Schrobilgen, G. J. *Inorg. Chem.* **1991**, *30*, 2540−2547.
(13) Sekar, P.; Ibers, J. A. *Inorg. Chem.* **2004**, *43*, 5436−5441.
(14) Ansari, M. A.; Ibers, J. A. *Coord. Chem. Rev.* **1990**, *100*, 223−266.
(15) Sheldrick, W. S.; Wachhold, M. *Coord. Chem. Rev.* **1998**, *176*, 211−322.
(16) Roof, L. C.; Kolis, J. W. *Chem. Rev.* **1993**, *93*, 1037−1080.
(17) Ansari, M. A.; McConnachie, J. M.; Ibers, J. A. *Acc. Chem. Res.* **1993**, *26*, 574−578.
(18) Simonnet-Jégat, C.; Sécheresse, F. *Chem. Rev.* **2001**, *101*, 2601−2611.
(19) Draganjac, M.; Rauchfuss, T. B. *Angew. Chem., Int. Ed. Engl.* **1985**, *24*, 742−757.

10.1021/ic0483646 CCC: $30.25
Published on Web 04/21/2005

ring compounds of Ti[24] and Ru.[25] Also known are the ten-membered $[Au(\mu\text{-}S_4)_2Au]^{2-}$ ring[26] and the unsymmetrically bridged compounds $[(ReCp(CO))_2(\mu\text{-}S_2)(\mu\text{-}S_3)]$[27] and $[Re_2(\mu_2\text{-}S)_2(\mu_2\text{-}S_3)_2(S_4)_2]\cdot 4H_2O$.[28] A number of compounds with the $M(\mu_2\text{-}S_2)(\mu_2\text{-}S)_2M$ core have also been reported, where M = V,[29,30] Fe,[31−34] Ru,[35] and Cr.[36]

Almost all such known chalcogen-bridged compounds are sulfides. The Se-containing compounds $[Re_2O_2Cp^*_2(\mu_2\text{-}Q)(\mu_2\text{-}Q_2)]$ (Q = S, Se)[37] and $[(Ti(MeCp)_2)_2(\mu\text{-}Se_2)_2]$[38] are known. Insofar as we know the only Te-containing compound of this type is $[(TiCp^*_2)_2(\mu\text{-}Te_2)_2]$.[39] Here, we report the syntheses and structural characterization of $[RuCp(PPh_3)(\mu_2\text{-}Se_2)]_2$ (**1**), $[Ru_2Cp_2(\mu_3\text{-}Se_2)(\mu_3\text{-}Se)]_2$ (**2**), $[(RuCp(PPh_3))_2(\mu_2\text{-}(1,4\text{-}\eta\text{:}3,6\text{-}\eta)Te_6)]$ (**3**), and $[(RuCp(PPh_3))_2(\mu_2\text{-}(1,4\text{-}\eta\text{:}3,6\text{-}\eta)Te_6)]\cdot CH_2Cl_2$ (**4**). The compound $[Ru(MeCp)(PPh_3)(\mu_2\text{-}Se_2)]_2[OTf]_2$ was characterized previously from its spectra,[40] but no crystal structure was reported.

Experimental Section

General Procedures. All experiments were carried out under an N_2 atmosphere with the use of Schlenk-line techniques. $Na_2[TeSe_3]$ and K_2Te were synthesized by the reactions of stoichiometric quantities of the elements in liquid NH_3. Te powder (Aldrich Chemical Co., Milwaukee, WI), Se powder (Cerac, Inc., Milwaukee, WI), and $[RuClCp(PPh_3)_2]$ (Strem Chemicals, Inc., Newburyport, ME) were used as received. CH_2Cl_2 (Fisher Chemicals, Inc., Fair Lawn, NJ) was dried over P_2O_5; anhydrous Et_2O (Fisher) was dried over Na/benzophenone; and DMF (Fisher) was dried over molecular sieves. NMR data were recorded on a Mercury 400 MHZ spectrometer. Elemental analyses were performed by Oneida Research Services, Whitesboro, NY. Samples for NMR analyses were washed with hexanes and then predried overnight under vacuum at 70 °C.

Synthesis of $[RuCp(PPh_3)(\mu_2\text{-}Se_2)]_2$ (1). $Na_2[TeSe_3]$ (113 mg, 0.28 mmol) was dissolved in 5 mL of DMF. To this brown solution 100 mg (0.14 mmol) of solid $[RuClCp(PPh_3)_2]$ was added. The resulting solution was stirred under an N_2 atmosphere for 3 h. It was then filtered through a cannula. The resultant filtrate was carefully layered with 10 mL of Et_2O and sealed. In 5 days 26 mg (32% yield) of $[RuCp(PPh_3)(\mu_2\text{-}Se_2)]_2$ was obtained as green needle-shaped crystals suitable for X-ray diffraction studies. For chemical analysis, crystals of **1** were dissolved in CH_2Cl_2, the solution was filtered through silica, and then **1** was precipitated by addition of hexane. The resultant analysis is consistent with a hexane solvate. Anal. Calcd for $C_{46}H_{40}P_2Ru_2Se_4\cdot C_6H_{14}$: C 49.61; H 4.32. Found: C 50.08; H 4.54. ^1H NMR ($CDCl_3$): δ 4.61 (s, 10 H), 7.23−7.26 (m, 30 H).

Synthesis of $[Ru_2Cp_2(\mu_3\text{-}Se_2)(\mu_3\text{-}Se)]_2$ (2). The same procedure used to obtain **1** was followed except that the layered filtrate was not sealed but rather was capped with a septum. In two weeks, in addition to green crystals of compound **1**, a few dark-brown X-ray quality crystals of $[Ru_2Cp_2(\mu_3\text{-}Se_2)(\mu_3\text{-}Se)]_2$ (**2**) were isolated.

Synthesis of $[(RuCp(PPh_3))_2(\mu_2\text{-}(1,4\text{-}\eta\text{:}3,6\text{-}\eta)Te_6)]$ (3). K_2Te (28 mg, 0.14 mmol) and Te (54 mg, 0.42 mmol) were stirred in 5 mL of DMF to give a purple solution. To this solution solid $[RuClCp(PPh_3)_2]$ (100 mg, 0.14 mmol) was added. The resulting solution was stirred under an N_2 atmosphere for 3 h. It was then filtered through a cannula. The resultant filtrate was carefully layered with 10 mL of Et_2O and the filtrate flask was sealed. After one week 55 mg, 0.034 mmol (49% yield) of $[(RuCp(PPh_3))_2(\mu_2\text{-}(1,4\text{-}\eta\text{:}3,6\text{-}\eta)Te_6)]$ (**3**) was obtained as brown needle-shaped crystals suitable for X-ray diffraction studies. Anal. Calcd for $C_{46}H_{40}P_2Ru_2Te_6$: C, 34.05; H 2.48. Found: C, 33.16; H 2.64. ^1H NMR ($CDCl_3$): δ 4.48 (s, 10 H), 7.26−7.34 (m, 30 H).

Synthesis of $[(RuCp(PPh_3))_2(\mu_2\text{-}(1,4\text{-}\eta\text{:}3,6\text{-}\eta)Te_6)]\cdot CH_2Cl_2$ (4). K_2Te (56 mg, 0.27 mmol) and Te (70 mg, 0.54 mmol) were stirred in 5 mL of DMF to give a purple polytelluride solution. $[RuClCp(PPh_3)_2]$ (70 mg, 0.10 mmol) was dissolved in 3 mL of CH_2Cl_2 and added dropwise to the polytelluride solution. The resulting solution was stirred under N_2 for 3 h and then filtered through a cannula. The filtrate was layered with 10 mL of Et_2O. After one week 28 mg, 0.016 mmol (32% yield) of $[(RuCp(PPh_3))_2(\mu_2\text{-}(1,4\text{-}\eta\text{:}3,6\text{-}\eta)Te_6)]\cdot CH_2Cl_2$ (**4**), the CH_2Cl_2 solvate of compound **3**, was obtained as brown needle-shaped crystals suitable for X-ray diffraction studies. Anal. Calcd for $C_{47}H_{42}Cl_2P_2Ru_2Te_6$: C, 33.06; H 2.48. Found: C, 32.72; H 2.37. ^1H NMR ($CDCl_3$): δ 4.48 (s, 10 H), 5.30 (s, 2H), 7.26−7.34 (m, 30 H).

X-ray Structure Determinations. Single-crystal X-ray diffraction data were collected with the use of graphite-monochromatized Mo Kα radiation (λ = 0.71073 Å) at 153 K on a Bruker Smart-1000 CCD diffractometer.[41] The crystal-to-detector distance was 5.023 cm. Crystal decay was monitored by recollecting 50 initial frames at the end of data collection. Data were collected by a scan of 0.3° in ω in four sets of 606 frames at φ settings of 0, 90, 180, and 270°. The exposure times were 15 s/frame. The collection of the intensity data was carried out with the program SMART.[41] Cell refinement and data reduction were carried out with the use of the

(20) Pleus, R. J.; Saak, W.; Pohl, S. *Z. Anorg. Allg. Chem.* **2001**, *627*, 250−253.
(21) Amarasekera, J.; Rauchfuss, T. B.; Rheingold, A. L. *Inorg. Chem.* **1987**, *26*, 2017−2018.
(22) Treichel, P. M.; Crane, R. A.; Haller, K. J. *Polyhedron* **1990**, *9*, 1893−1899.
(23) Giolando, D. M.; Rauchfuss, T. B.; Rheingold, A. L.; Wilson, S. R. *Organometallics* **1987**, *6*, 667−675.
(24) Bolinger, C. M.; Rauchfuss, T. B.; Wilson, S. R. *J. Am. Chem. Soc.* **1981**, *103*, 5620−5621.
(25) Brunner, H.; Janietz, N.; Wachter, J.; Nuber, B.; Ziegler, M. L. *J. Organomet. Chem.* **1988**, *356*, 85−91.
(26) Müller, A.; Römer, M.; Bögge, H.; Krickemeyer, E.; Schmitz, K. *Inorg. Chim. Acta* **1984**, *85*, L39−L41.
(27) Herberhold, M.; Reiner, D. *Z. Naturforsch. B: Anorg. Chem. Org. Chem.* **1984**, *39*, 1199−1205.
(28) Müller, A.; Krickemeyer, E.; Wittneben, V.; Bögge, H.; Lemke, M. *Angew. Chem., Int. Ed. Engl.* **1991**, *30*, 1512−1514.
(29) Herberhold, M.; Kuhnlein, M. *New J. Chem.* **1988**, *12*, 357−359.
(30) Bolinger, C. M.; Rauchfuss, T. B.; Rheingold, A. L. *J. Am. Chem. Soc.* **1983**, *105*, 6321−6323.
(31) Brunner, H.; Janietz, N.; Meier, W.; Sergeson, G.; Wachter, J.; Zahn, T.; Ziegler, M. L. *Angew. Chem., Int. Ed. Engl.* **1985**, *24*, 1060−1061.
(32) Weberg, R.; Haltiwanger, R. C.; DuBois, M. R. *Organometallics* **1985**, *4*, 1315−1318.
(33) Weberg, R. T.; Haltiwanger, R. C.; DuBois, M. R. *New J. Chem.* **1988**, *12*, 361−371.
(34) Yamada, M.; Tobita, H.; Inomata, S.; Ogino, H. *Bull. Chem. Soc. Jpn.* **1996**, *69*, 861−867.
(35) Rauchfuss, T. B.; Rodgers, D. P. S.; Wilson, S. R. *J. Am. Chem. Soc.* **1986**, *108*, 3114−3115.
(36) Goh, L. Y.; Mak, T. C. W. *J. Chem. Soc., Chem. Commun.* **1986**, 1474−1475.
(37) Herberhold, M.; Jin, G.-X.; Milius, W. *J. Organomet. Chem.* **1993**, *459*, 257−263.
(38) Giolando, D. M.; Papavassiliou, M.; Pickardt, J.; Rauchfuss, T. B.; Steudel, R. *Inorg. Chem.* **1988**, *27*, 2596−2600.
(39) Fenske, D.; Grissinger, A. *Z. Naturforsch. B: Chem. Sci.* **1990**, *45b*, 1309−1313.
(40) Amarasekera, J.; Houser, E. J.; Rauchfuss, T. B.; Stern, C. L. *Inorg. Chem.* **1992**, *31*, 1614−1620.
(41) *Bruker SMART Version 5.054 Data Collection and SAINT-Plus Version 6.45a Data Processing Software for the SMART System*; Bruker Analytical X-ray Instruments, Inc.: Madison, WI, 2003.

Table 1. Selected Crystallographic Data for $[RuCp(PPh_3)(\mu_2\text{-}Se_2)]_2$ (**1**), $[Ru_2Cp_2(\mu_3\text{-}Se_2)(\mu_3\text{-}Se)]_2$ (**2**), $[(RuCp(PPh_3))_2(\mu_2\text{-}(1,4\text{-}\eta\text{:}3,6\text{-}\eta)Te_6)]$ (**3**), and $[(RuCp(PPh_3))_2(\mu_2\text{-}(1,4\text{-}\eta\text{:}3,6\text{-}\eta)Te_6)]\cdot CH_2Cl_2$ (**4**)

	1	**2**	**3**	**4**
formula	$C_{46}H_{40}P_2Ru_2Se_4$	$C_{20}H_{20}Ru_4Se_6$	$C_{46}H_{40}P_2Ru_2Te_6$	$C_{47}H_{42}Cl_2P_2Ru_2Te_6$
formula weight	1172.7	1138.4	1622.46	1707.39
crystal system	triclinic	monoclinic	monoclinic	triclinic
space group	$P\bar{1}$	$C2/c$	$C2/c$	$P\bar{1}$
a (Å)	9.5419(14)	12.401(3)	25.211(2)	9.3753(16)
b (Å)	11.8807(17)	13.607(3)	13.8374(12)	14.520(2)
c (Å)	11.9229(18)	14.801(3)	17.1079(15)	19.117(3)
α (deg)	93.561(3)	90	90	81.536(3)
β (deg)	93.604(3)	110.628(3)	119.5060(10)	83.552(3)
γ (deg)	109.951(2)	90	90	74.870(3)
V	1263.0(3)	2337.5(8)	5194.2(8)	2477.5(7)
T (K)	153	153	153	153
Z	1	4	4	2
$\rho_{calc.}$ (g cm^{-3})	1.542	3.235	2.075	2.289
μ (Mo Kα) (mm^{-1})	3.57	11.886	3.975	4.277
$R_1(F_o)$ ($F_o^2 > 2\sigma(F_o^2)$)[a]	0.0443	0.0347	0.0426	0.0496
$wR(F_o^2)$[b]	0.1295	0.0860	0.1022	0.1459

[a] $R_1(F_o) = \sum||F_o| - |F_c||/\sum|F_o|$. [b] $wR(F_o^2) = [\sum w(F_o^2 - F_c^2)^2/\sum wF_o^4]^{1/2}$; $w^{-1} = \sigma^2(F_o^2) + (qF_o^2)^2$ for $F_o^2 > 0$; $w^{-1} = \sigma^2(F_o^2)$ for $F_o^2 \le 0$; $q = 0.068$ for **1**; 0.038 for **2**; 0.056 for **3**; 0.087 for **4**.

program SAINT[41] and face-indexed absorption corrections were performed numerically with the use of the program XPREP.[42] Then the program SADABS[41] was employed to make incident beam and decay corrections.

The structures were solved with the direct methods program SHELXS and refined with the full-matrix least-squares program SHELXL of the SHELXTL suite of programs.[42] The positions of the hydrogen atoms were idealized and constrained with the use of a riding model. The final models involved anisotropic displacement parameters for all non-hydrogen atoms. The solution and refinement of the structures of **2** and **4** were straightforward. However, the structures of compounds **1** and **3** both exhibited residual electron density ascribable to solvent that could not be modeled satisfactorily. Consequently, the program SQUEEZE[43] of the PLATON program suite was used to model these solvent regions. These amounted to 153 electrons per unit cell of compound **1**, corresponding to about four DMF molecules per Ru_2Se_4 unit, and 110 electrons per unit cell of compound **3**, corresponding to about three DMF molecules per Ru_2Te_6 unit. The presence of these solvents is not taken into account in the formulas of **1** or **3** or in the associated crystal data of Table 1. In compound **1** one of the phenyl rings exhibits displacement ellipsoids suggestive of some positional disorder. Additional details may be found in the Supporting Information.

Electronic Structure Calculations. Calculations were performed on compounds **3** and **4** with the use of first principles density functional theory (DFT). For comparison, we also performed calculations on the two S-analogues $[(RuCp(P(OMe)_3))_2(\mu_2\text{-}S_6)]$[22] and $[(Ru(MeCp)(PPh_3))_2(\mu_2\text{-}S_6)]$.[21] Single-point energy calculations with experimental geometries were performed; these were carried out with the Amsterdam density functional program (ADF2003).[44−46] The exchange-correlation potentials were treated in the local density approximation (LDA) by means of the Vosko−Wilk−Nusair (VWN) correlation scheme.[47] The TZP numerical basis set was used. It is of high quality, comparable to the best Gaussian bases available. For all atoms a triple-ζ Slater-type orbital (STO) basis set augmented by one polarization function was employed. The frozen core approximation was used to treat the core electrons. Bond and valency indices were calculated according to the definitions proposed by Mayer[48,49] with a program[50,51] designed for ADF output files. The Xaim program[52] was used to search bond critical points according to the atoms-in-molecules theory of Bader.[53]

Two distinct types of charge distribution analyses were made: by analytic Mulliken atomic orbital populations, and by Voronoi volume charge analysis. The two analyses give a complementary and reinforcing view of the electronic distribution. The traditional Mulliken atomic population analysis of the occupied orbitals is useful to extract effective atomic configurations, whereas the volume charge analysis exploits a partition of the space associated with each atom and an integration of the charge within each volume. The Voronoi volume of an atom used in the present analyses is defined as the region of space closest to that atom, being a polyhedron defined by planes bisecting interatomic vectors. The Mulliken method is more chemically intuitive, whereas the volume charge analysis is more attuned to concepts of ionic and covalent atomic radii. Neither of them is invariant to the choice of atomic parameters, namely to atomic orbital basis sets and the geometric definition of atomic volumes. However, the combination of the two methods leads to considerable insight into charge distributions.

Results and Discussion

In an effort to synthesize mixed Te/Se polychalcogenometalates we have chosen the $[TeSe_3]^{2-}$ ligand as the precursor owing to its use in the successful syntheses of the $[AuTeSe_2]_2^{2-}$ [54] and $[(CpM(\mu_2\text{-}Se_2))_3(\mu_3\text{-}O)(\mu_3\text{-}TeSe_3)]^-$ (M = Zr, Hf) anions.[55]

(42) Sheldrick, G. M. *SHELXTL Version 6.14*; Bruker Analytical X-ray Instruments, Inc.: Madison, WI, 2003.
(43) van der Sluis, P.; Spek, A. L. *Acta Crystallogr. Sect. A: Found. Crystallogr.* **1990**, *46*, 194−201.
(44) Te Velde, G.; Bickelhaupt, F. M.; Baerends, E. J.; Fonseca Guerra, C.; Van Gisbergen, S. J. A.; Snijders, J. G.; Ziegler, T. *J. Comput. Chem.* **2001**, *22*, 931−967.
(45) Baerends, E. J.; Ellis, D. E.; Ros, P. *Chem. Phys.* **1973**, *2*, 41−51.
(46) Guerra, C. F.; Snijders, J. G.; te Velde, G.; Baerends, E. J. *Theor. Chem. Acc.* **1998**, *99*, 391−403.
(47) Vosko, S. H.; Wilk, L.; Nusair, M. *Can. J. Phys.* **1980**, *58*, 1200−1211.
(48) Mayer, I. *Int. J. Quantum Chem.* **1986**, *XXIX*, 73−84.
(49) Mayer, I. *Int. J. Quantum Chem.* **1986**, *XXIX*, 477−483.
(50) Bridgeman, A. J.; Empson, C. J. *Mayer*; The University of Hull: Hull, U.K., 2003.
(51) Bridgeman, A. J.; Cavigliasso, G.; Ireland, L. R.; Rothery, J. *J. Chem. Soc., Dalton Trans.* **2001**, 2095−2108.
(52) Alba, J. C. O.; Jané, C. B. *Xaim, ver. 1.0*; Departament de Química Física i Inorgànica, Universitat Rovira i Virgili: Pl. Tarragona, Spain, 1998.
(53) Bader, R. F. W. *Atoms in Molecules: A Quantum Theory*; Clarendon Press: Oxford, 1990.
(54) Dibrov, S. M.; Ibers, J. A. *Chem. Commun.* **2003**, 2158−2159.

Table 2. Selected Bond Distances (Å) and Angles (deg) for $[RuCp(PPh_3)(\mu_2\text{-}Se_2)]_2$ (**1**)

Ru(1)−P(1)	2.281(2)	C−C (Cp)	1.401(10)−1.423(9)
Ru(1)−Se(2)	2.4114(8)	Se(2)−Ru(1)−Se(1)	102.67(3)
Ru(1)−Se(1)	2.4211(8)	Se(2A)−Se(1)−Ru(1)	103.40(3)
Se(1)−Se(2A)	2.3307(9)	Se(1A)−Se(2)−Ru(1)	107.83(3)
Ru(1)−C	2.228(6)−2.271(6)	Se(1)−Ru(1)−P(1)	90.36(5)
P(1)−C	1.831(6)−1.838(6)	Se(2)−Ru(1)−P(1)	89.45(5)
C−C (Ph)	1.353(11)−1.396(9)	Ru(1)−Se(2)−Se(1A)−Ru(1A)	71.7

Table 3. Selected Bond Distances (Å) and Angles (deg) for $[Ru_2Cp_2(\mu_3\text{-}Se_2)(\mu_3\text{-}Se)]_2$ (**2**)

Ru(1)−Se(2)	2.3924(9)	Se(1)−Ru(1)−Ru(2)	107.46(3)
Ru(1)−Se(1A)	2.4503(8)	Se(1A)−Ru(2)−Se(3)	92.72(3)
Ru(1)−Se(1)	2.4851(8)	Se(1A)−Ru(2)−Se(2)	98.07(3)
Ru(1)−Ru(2)	2.8250(8)	Se(3)−Ru(2)−Se(2)	87.56(3)
Ru(2)−Se(1A)	2.4133(8)	Se(1A)−Ru(2)−Ru(1)	55.10(2)
Ru(2)−Se(3)	2.4500(9)	Se(3)−Ru(2)−Ru(1)	117.00(3)
Ru(2)−Se(2)	2.4526(9)	Se(2)−Ru(2)−Ru(1)	53.35(2)
Se(2)−Se(3A)	2.3550(9)	Se(1A)−Ru(1)−Ru(2)	53.88(2)
Ru(1)−C	2.218(6)−2.262(6)	Ru(2A)−Se(1)−Ru(1A)	71.01(2)
Ru(2)−C	2.184(7)−2.275(7)	Ru(2A)−Se(1)−Ru(1)	121.28(3)
C−C	1.403(11)−1.427(10)	Ru(1A)−Se(1)−Ru(1)	105.46(3)
Se(2)−Ru(1)−Se(1A)	98.70(3)	Se(3A)−Se(2)−Ru(1)	112.76(3)
Se(2)−Ru(1)−Se(1)	94.40(3)	Se(3A)−Se(2)−Ru(2)	119.87(3)
Se(1A)−Ru(1)−Se(1)	73.95(3)	Ru(1)−Se(2)−Ru(2)	71.32(2)
Se(2)−Ru(1)−Ru(2)	55.33(2)	Se(2A)−Se(3)−Ru(2)	111.19(3)

$[RuCp(PPh_3)(\mu_2\text{-}Se_2)]_2$ (1). Reaction of $Na_2[TeSe_3]$ with $[RuClCp(PPh_3)_2]$ in DMF followed by slow addition of Et_2O afforded green needles of $[RuCp(PPh_3)(\mu_2\text{-}Se_2)]_2$ (**1**) in 32% yield. Compound **1** could also be obtained in moderate yield by the reaction of K_2Se_2 or K_2Se_3 with $[RuClCp(PPh_3)_2]$ under conditions similar to those described above. The MeCp analogue of compound **1** has been reported, but with no accompanying crystallographic information.[40] The molecular structure of $[RuCp(PPh_3)(\mu_2\text{-}Se_2)]_2$ (**1**) is depicted in Figure 1 and selected bond distances and angles are summarized in Table 2. In the structure, the two bridging Se_2 groups lead to a centrosymmetric Ru_2Se_4 six-membered core with a chair conformation. The bulky PPh_3 groups are in equatorial positions and the smaller Cp ligands are in axial positions. The Se−Se bond length is 2.3307(9) Å, typical for a single bond. The Ru−P bond length of 2.281(2) Å is also a normal single bond. All other bonds involving P or C are typical. Similar to its sulfur analogues $[Ru(MeCp)(PPh_3)(\mu_2\text{-}S_2)]_2$[21] and $[RuCp(P(OMe)_3)(\mu_2\text{-}S_2)]_2$,[22] compound **1**, $[RuCp(PPh_3)(\mu_2\text{-}Se_2)]_2$, is diamagnetic and has a symmetric structure, as evidenced by ^1H NMR spectroscopy. Ru−S multiple bonding was invoked to explain the diamagnetism of the sulfur analogues.[21,22] That Ru−Se multiple bonding occurs in $[RuCp(PPh_3)(\mu_2\text{-}Se_2)]_2$ is not clear from the Ru−Se bond lengths of 2.4114(8) Å and 2.4211(8) Å because direct comparisons with analogous compounds are lacking. However, in the compound $[Ru_2Cp_2(\mu_3\text{-}Se_2)(\mu_3\text{-}Se)]_2$ (**2**) described below, the Ru−Se bond lengths are 2.3924(9) Å, 2.4503(8) Å, and 2.4851(8) Å; in $[Ru(MeCp)(PPh_3)(\mu_2\text{-}(1\text{-}\eta^1\text{:}2\text{-}\eta^2)\text{-}Se_2)]_2^{2+}$[40] they are 2.473 (1) Å and 2.556(1) Å; and in $[\{RuCl_2(P(OMe)_3)_2\}(\mu_2\text{-}Se_2)(\mu\text{-}Cl)]_2$[56] they average 2.33 Å. Ru−Se multiple bonding is not supported by the first principles calculations described below.

$[Ru_2Cp_2(\mu_3\text{-}Se_2)(\mu_3\text{-}Se)]_2$ (2). A small amount of crystalline $[Ru_2Cp_2(\mu_3\text{-}Se_2)(\mu_3\text{-}Se)]_2$ (**2**) was obtained consistently if the system that led to the crystallization of **1** was capped with a septum, rather than sealed. Presumably **2** results from the exposure of the system to oxygen. Compound **2** was not obtained in sufficient yield to enable chemical analyses or spectroscopic studies to be performed. The structure of **2** contains a centrosymmetric Ru_4Se_6 cluster formed from the two bridging Se groups and the two bridging Se_2 groups. Each Ru is π-bonded to a Cp ring (Figure 2). Selected bond distances and angles are given in Table 3. There appear to be no chalcogen/metal analogues of compound **2**. It is an

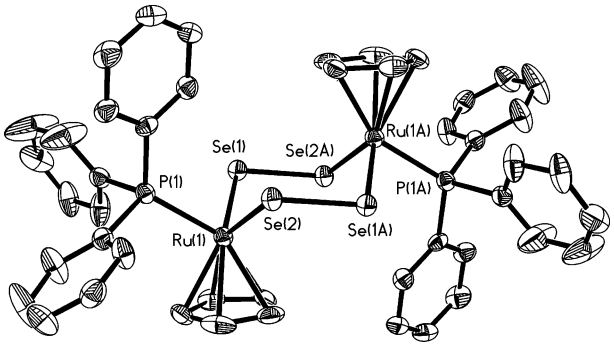

Figure 1. Structure of $[RuCp(PPh_3)(\mu_2\text{-}Se_2)]_2$ (**1**).

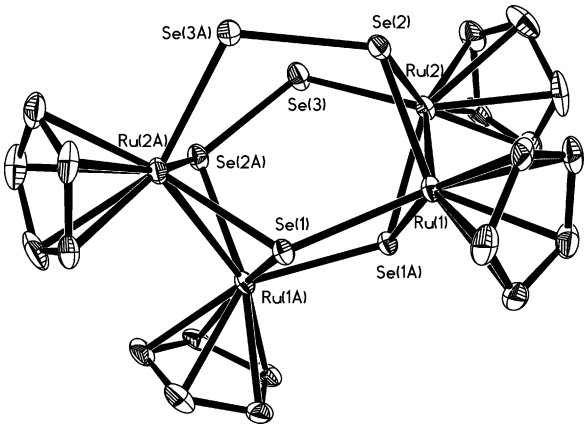

Figure 2. Structure of $[Ru_2Cp_2(\mu_3\text{-}Se_2)(\mu_3\text{-}Se)]_2$ (**2**).

(55) Dibrov, S. M.; Ibers, J. A. *C. R. Chimie* **2005**, in press.
(56) Mizutani, J.; Matsumoto, K. *Chem. Lett.* **2000**, *29*, 72−73.

Table 4. Selected Bond Distances (Å) and Angles (deg) for $[(RuCp(PPh_3))_2(\mu_2\text{-}(1,4\text{-}\eta\text{:}3,6\text{-}\eta)Te_6)]$ (**3**)

Ru(1)−Te(1)	2.5940(6)	Ru(1)−Te(3A)	2.6458(6)
Te(1)−Te(2)	2.7975(6)	Te(1)−Te(1A)	2.9493(8)
Te(2)−Te(3)	2.7228(6)	Te(3)−Ru(1A)	2.6458(6)
Ru(1)−P(1)	2.284(2)	P(1)−C	1.833(6)−1.849(6)
Ru−C	2.195(7)−2.231(6)	C−C (Ph)	1.369(10)−1.405(9)
Te(1)−Ru(1)−Te(3A)	93.37(2)	C−C (Cp)	1.402(10)−1.421(9)
Ru(1)−Te(1)−Te(1A)	108.43(2)	Ru(1)−Te(1)−Te(2)	108.77(2)
Te(3)−Te(2)−Te(1)	89.90(2)	Te(2)−Te(1)−Te(1A)	94.96(2)
		Ru(1A)−Te(3)−Te(2)	98.87(2)

Table 5. Selected Bond Distances and Angles for $[(RuCp(PPh_3))_2(\mu_2\text{-}(1,4\text{-}\eta\text{:}\ 3,6\text{-}\eta)Te_6)]\cdot CH_2Cl_2$ (**4**)

Ru(1)−Te(4)	2.562(1)	Ru(1)−Te(1)	2.638(1)
Ru(2)−Te(3)	2.563(1)	Ru(2)−Te(6)	2.651(1)
Te(1)−Te(2)	2.716(1)	Te(2)−Te(3)	2.740(1)
Te(3)−Te(4)	3.046(1)	Te(4)−Te(5)	2.725(1)
Te(5)−Te(6)	2.706(1)	Ru(1)−P(1)	2.294(3)
Ru(2)−P(2)	2.284(3)	Ru(1)−C	2.20(1)−2.24(1)
Ru(2)−C	2.20(1)−2.25(1)	C−C (Ph and Cp)	1.35(2)−1.44(2)
P−C	1.83(1)−1.85(1)	Te(3)−Ru(2)−Te(6)	96.62(3)
Te(4)−Ru(1)−Te(1)	94.90(4)	Te(1)−Te(2)−Te(3)	91.71(3)
Ru(1)−Te(1)−Te(2)	103.95(3)	Ru(2)−Te(3)−Te(4)	109.06(3)
Ru(2)−Te(3)−Te(2)	104.95(3)	Ru(1)−Te(4)−Te(5)	105.40(3)
Te(2)−Te(3)−Te(4)	88.50(3)	Te(5)−Te(4)−Te(3)	90.44(3)
Ru(1)−Te(4)−Te(3)	111.48(3)	Ru(2)−Te(6)−Te(5)	102.79(3)
Te(6)−Te(5)−Te(4)	91.34(3)		

electron-paired compound and therefore it should be diamagnetic. The two Ru(III) atoms in each pair are joined by a normal 2.8250(8) Å single bond. The Ru−μ_3-Se distance of 2.4851(8) Å is longer than the Ru−μ_3-Se_2 distances of 2.3924(9) and 2.4503(8) Å. The Se−Se distance of 2.3550(9) Å is a normal single bond. Ru−C and C−C distances are typical.

$[(RuCp(PPh_3))_2(\mu_2\text{-}(1,4\text{-}\eta\text{:}3,6\text{-}\eta)Te_6)]$ (3) and $[(RuCp(PPh_3))_2(\mu_2\text{-}(1,4\text{-}\eta\text{:}3,6\text{-}\eta)Te_6)]\cdot CH_2Cl_2$ (4). Because the reaction of $[RuClCp(PPh_3)_2]$ with $Na_2[TeSe_3]$ afforded only Se-containing products, the reaction of $[RuClCp(PPh_3)_2]$ with Na_2Te under similar conditions was investigated. If DMF was used as solvent then the compound $[(RuCp(PPh_3))_2(\mu_2\text{-}(1,4\text{-}\eta\text{:}\ 3,6\text{-}\eta)Te_6)]$ (**3**) was obtained in 49% yield; if DMF/CH_2Cl_2 was the solvent system, then $[(RuCp(PPh_3))_2(\mu_2\text{-}(1,4\text{-}\eta\text{:}3,6\text{-}\eta)Te_6)]\cdot CH_2Cl_2$ (**4**) was obtained in 32% yield. In compound **3** (Figure 3) and its CH_2Cl_2 solvate (Figure 4) the Ru centers are bound to a bridging Te_6 chain at the 1, 4, 3, and 6 positions, leading to a bicyclic Ru_2Te_6 ring. The rings in these two compounds are shown in Figure 5 and additional metrical data are provided in Tables 4 and 5. Insofar as we can determine there are no other examples of a bicyclic complex where fusion occurs along a Te−Te bond.

In the closely related S-analogues $[(RuCp(P(OMe)_3))_2(\mu_2\text{-}S_6)]$[22] and $[(Ru(MeCp)(PPh_3))_2(\mu_2\text{-}S_6)]$[21] the S−S bond lengths at the ring fusion are 2.610(2) and 2.772(3) Å, respectively. That these two lengths differ so much is perhaps surprising and may point to the general ease of deformation of the bicyclic ring depending on the environment. These S−S bond lengths at the postulated ring fusion are around 0.5−0.6 Å longer than a normal single bond. Nevertheless, S−S bonding was invoked in $[(Ru(MeCp)(PPh_3))_2(\mu_2\text{-}S_6)]$[21] to rationalize the diamagnetism of the compounds; it was believed to be induced by multiple Ru−S bonding. Similarly, a theoretical study[57] of $[(RuCp(P(OMe)_3))_2(\mu_2\text{-}S_6)]$[22] suggested delocalization of charge in the molecular LUMO that

(57) Kanis, D. R. Ph.D. Thesis, University of Wisconsin-Madison. 1989.

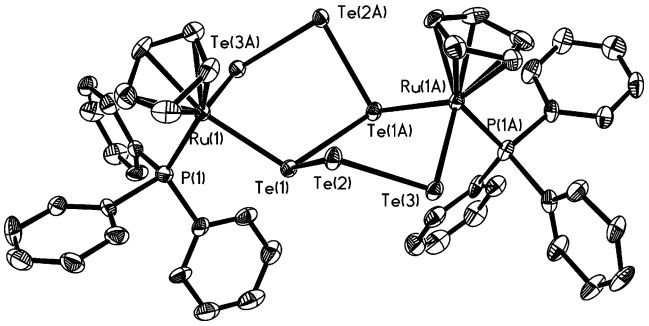

Figure 3. Structure of $[(RuCp(PPh_3))_2(\mu_2\text{-}(1,4\text{-}\eta\text{:}3,6\text{-}\eta)Te_6)]$ (**3**).

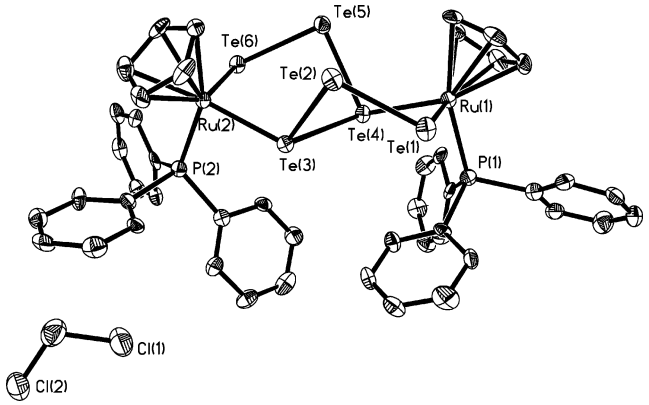

Figure 4. Structure of $[(RuCp(PPh_3))_2(\mu_2\text{-}(1,4\text{-}\eta\text{:}3,6\text{-}\eta)Te_6)]\cdot CH_2Cl_2$ (**4**).

involves multiple Ru−S bonding and antibonding character between the S atoms in the ring. The present results support the delocalization of charge on those Ru_2S_6 rings, but do not agree with the multiple Ru−S bonding interpretations. Compounds **3** and **4** are also diamagnetic, which has been confirmed by spin-polarized calculations. For these compounds the case for ring fusion is much stronger. At ring fusion the Te−Te bond lengths are 2.9493(8) and 3.046(1) Å, respectively. (Note that here also the length is sensitive to the environment.) In acyclic Te_n^{2-} species, Te−Te bond lengths range from about 2.68 to about 2.86 Å.[10] Thus, the Te−Te bond lengths at the ring fusion are perhaps 0.2 Å

Table 6. Mulliken Atomic Charges and Volume-Integrated Charges (e^-) of $[(RuCp(PPh_3))_2(\mu_2\text{-}(1,4\text{-}\eta\text{:}3,6\text{-}\eta)Te_6)]$ (**3**)

group	Mulliken charge	Voronoi charge
Ru(1)	−0.05	0.55
Te(1)	0.09	0.35
Te(2)	−0.08	0.15
Te(3)	0.06	0.20
Ru_2Te_6	0.02	2.49
Cp	−0.30	−0.94
PPh_3	0.29	−0.32

Table 7. Mulliken Atomic Charges and Volume-Integrated Charges (e^-) of $[(RuCp(PPh_3))_2(\mu_2\text{-}(1,4\text{-}\eta\text{:}3,6\text{-}\eta)Te_6)]\cdot CH_2Cl_2$ (**4**)

group	Mulliken charge	Voronoi charge
Ru(1)	−0.05	0.56
Ru(2)	−0.08	0.54
Te(1)	0.04	0.14
Te(2)	−0.05	0.08
Te(3)	0.13	0.36
Te(4)	−0.02	0.45
Te(5)	−0.02	0.10
Te(6)	−0.00	0.26
Ru_2Te_6	−0.04	2.48
Cp(1)	−0.27	−0.88
Cp(2)	−0.25	−0.89
PPh_3(1)	0.29	−0.36
PPh_3(2)	0.28	−0.34

Table 8. Mulliken Atomic Charges and Volume-Integrated Charges (e^-) of $[(Ru(MeCp)(PPh_3))_2(\mu_2\text{-}S_6)]$

group	Mulliken charge	Voronoi charge
Ru(1)	0.38	0.93
Ru(2)	0.49	0.95
S(1)	−0.09	−0.07
S(2)	0.01	0.06
S(3)	−0.19	−0.21
S(4)	−0.19	−0.14
S(5)	−0.00	0.08
S(6)	−0.19	−0.01
Ru_2S_6	0.22	1.59
MeCp(1)	−0.31	−0.66
MeCp(2)	−0.28	−0.72
PPh_3 (2)	0.20	−0.12
PPh_3 (2)	0.17	−0.11

Table 9. Mulliken Atomic Charges and Volume-Integrated Charges (e^-) of $[(RuCp(P(OMe)_3))_2(\mu_2\text{-}S_6)]$

Group	Mulliken charge	Voronoi charge
Ru(1)	0.43	0.94
Ru(2)	0.39	0.94
S(1)	−0.18	−0.08
S(2)	0.02	0.03
S(3)	−0.23	−0.13
S(4)	−0.16	−0.01
S(5)	0.04	0.04
S(6)	−0.21	−0.21
Ru_2S_6	0.10	1.52
Cp(1)	−0.27	−0.64
Cp(2)	−0.24	−0.63
$P(OMe)_3$ (1)	0.22	−0.67
$P(OMe)_3$ (2)	0.19	−0.12

longer than a normal single bond. The Ru−Te bond lengths range from 2.562(1) to 2.651(1) Å. Owing to the paucity of other examples, it is difficult to argue from structural results that these bonds indicate multiple bond character. Nevertheless, they are shorter than the Ru−Te bonds of 2.673(2) to 2.745(2) Å in the Te−Te−Ru−Te−Te fragments in $[PPh_4]_2[Ru_6(Te_2)_7(CO)_{12}]$[58] and $[PPh_4]_2[Ru_4(Te_2)_2(Te)_2(TeMe)_2(CO)_8]$.[59]

(58) Huang, S.-P.; Kanatzidis, M. G. *J. Am. Chem. Soc.* **1992**, *114*, 5477−5478.

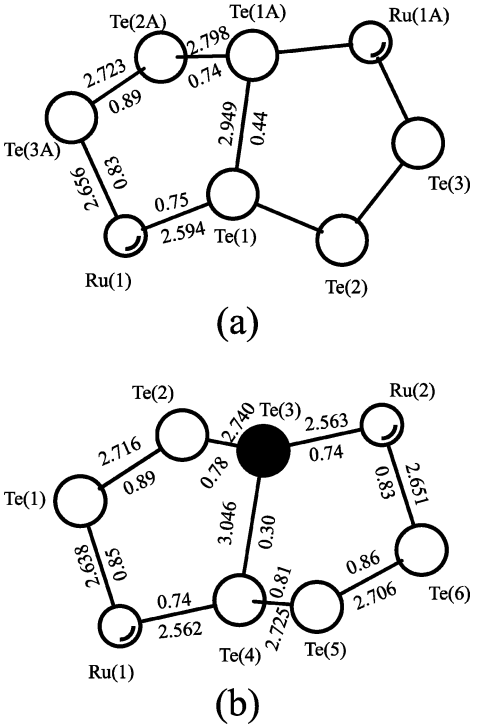

Figure 5. Bond distances and bond orders of the bicyclic Ru_2Te_6 rings in (a) $[(RuCp(PPh_3))_2(\mu_2\text{-}(1,4\text{-}\eta\text{:}3,6\text{-}\eta)Te_6)]$ (**3**) and (b) $[(RuCp(PPh_3))_2(\mu_2\text{-}(1,4\text{-}\eta\text{:}3,6\text{-}\eta)Te_6)]\cdot CH_2Cl_2$ (**4**).

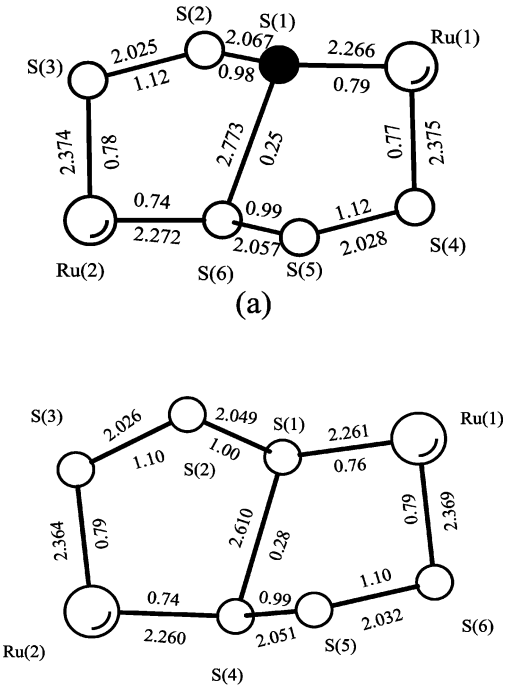

Figure 6. Bond distances (from CSD-FORBUJ) and bond orders of the Ru_2S_6 ring in (a) $[(Ru(MeCp)(PPh_3))_2(\mu_2\text{-}S_6)]$[21] and (b) $[(RuCp(P(OMe)_3))_2(\mu_2\text{-}S_6)]$.[22]

Charge Distributions. Tables 6 and 7 show the Mulliken atomic charges and volume-integrated atomic charges for Te_6-containing compounds **3** and **4**. According to the Mulliken analysis, charges on the Ru and Te atoms are

(59) Das, B. K.; Kanatzidis, M. G. *Inorg. Chem.* **1995**, *34*, 1011−1012.

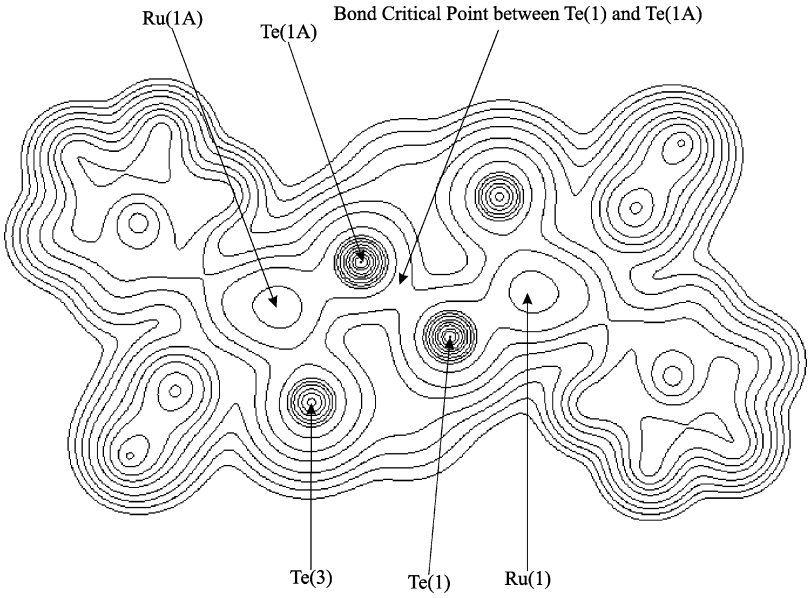

Figure 7. Valence charge density contour map within Te(1)−Te(1A)−Te(3) plane in $[(RuCp(PPh_3))_2(\mu_2\text{-}(1,4\text{-}\eta\text{:}3,6\text{-}\eta)Te_6)]$ (**3**). Equal interval contours are shown.

approximately zero, which results in a nearly neutral bicyclic Ru_2Te_6 ring. The Mulliken charges on the Cp ligands are also rather small, ranging from −0.25 to −0.30 e^-. The corresponding charge distributions for the S-analogues are listed in Tables 8 and 9. The Mulliken charges on Cp or MeCp ligands of the S-analogues range from −0.24 to −0.31 e^-, which are comparable to those in compounds **3** and **4**. The Ru atoms of the Ru_2S_6 rings bear more positive charge than those of the Ru_2Te_6 rings, because the electronegativity of Te (2.01) is much less than that of S (2.44). To understand better the spatial electronic charge distributions, the volume-integrated charges were also calculated. Because the boundary planes of Voronoi cells are defined to be halfway between atoms without regard to atomic radii, the Voronoi analysis often leads to charges that are not chemically intuitive and that differ significantly from those obtained in the Mulliken analysis. For example, the volume charges of Ru are 0.55 to 0.56 e^- in the Te-compounds and 0.93 to 0.94 e^- in the S-compounds, tracking the trend in Mulliken charges (−0.05 to −0.08 e^- with Te-compounds and 0.38 to 0.49 e^- with S-compounds). The Voronoi cells are too compact to represent the anionic character of Te accurately; the Te charges vary from +0.08 to +0.45 e^-. The volume analysis of the smaller S anion gives results more consistent with the corresponding Mulliken charges. The volume charges on the Ru_2Te_6 rings are 2.49 e^- and 2.48 e^- in compounds **3** and **4**, respectively, versus those of 1.59 e^- and 1.52 e^- on the Ru_2S_6 rings in the S-analogues.[21,22] Thus, the compact Voronoi cells for Te give an exaggerated cationic character to the Ru_2Te_6 rings compared to the Ru_2S_6 rings, in contradiction to the Mulliken analysis. Owing to the exclusion of density from the Te Voronoi cells the volume charges on the ligands in compound **3** and **4** are also larger than those on the related ligands in the two S-analogues, in disagreement with the Mulliken analysis.

Spin polarized configurations of these four compounds were found to be unstable, decaying to the spin-restricted states. After self-consistent field iterations, spin moments on the Ru atoms tended to zero, which is consistent with their observed diamagnetism.

Bond Analysis. Mayer bond order indices for Ru_2Te_6 in compounds **3** and **4** are given in Figure 5. Bonding interactions exist between the bridging Te atoms. Bond orders are 0.44 e^- for the Te(1)−Te(1A) bond in compound **3** and 0.30 e^- for the Te(3)−Te(4) bond in compound **4**, indicative of significant shared bonding charge of about $^2/_3$ of that found for Te−Te single bonds. Bond orders for other bonds along the Ru_2Te_6 rings range from 0.74 to 0.89 e^-, indicative of the absence of multiple bonding character. A plot of Te−Te bond order (B) versus bond length (R) reveals a reasonably linear correlation, with d*B*/d*R* about −1.73 e^-/Å. No similar correlation was found for Ru−Te bond order versus distance; we presume this is because of the strong dependence of such a correlation on angular Ru−Te bond distortions around the metal site. Figure 6 shows the bond distances and bond orders of the two Ru_2S_6 rings in the S-analogues. Bond orders for the bridging S−S bonds are 0.25 and 0.28 e^-, somewhat smaller than those for the bridging Te−Te bonds. There is no indication of multiple bonding interactions in the Ru_2S_6 rings, contrary to previous suggestions for $(Ru(MeCp)(PPh_3))_2(\mu_2\text{-}S_6)$.[21] The bond orders for other bonds along the Ru_2S_6 rings range from 0.74 to 1.12 e^- for $(Ru(MeCp)(PPh_3))_2(\mu_2\text{-}S_6)$ and from 0.74 to 1.10 e^- for $(RuCp(P(OMe)_3))_2(\mu_2\text{-}S_6)$. A plot of S−S bond order (B) versus bond length (R) leads to a reasonably linear correlation, with d*B*/d*R* about −1.19 e^-/Å.

Figure 7 shows a contour map of the electron density within the Te(1)−Te(1A)−Te(3) plane in compound **3**. The bond critical point between Te(1)−Te(1A) has two negative curvatures and one positive curvature is therefore a (3, −1) critical point.[47] Other Ru−Te or Te−Te bonds on the Ru_2Te_6 rings are also (3, −1) critical points. The two negative curvatures of (3, −1) critical points are perpendicular to the bond path, where charge densities are local maxima. The

Table 10. Selected Bond Properties at Bond Critical Points ($\nabla\rho(r_c) = 0$)[a], and Laplacian Curvature for [(RuCp(PPh$_3$))$_2$(μ_2-(1,4-η:3,6-η)Te$_6$)] (**3**), and [(RuCp(PPh$_3$))$_2$(μ_2-(1,4-η:3,6-η)Te$_6$)]-CH$_2$Cl$_2$ (**4**)

bond	bond distances (Å)	$\rho(r_c)$(e$^-$/au^3)	$\nabla^2\rho(r_c)$(e$^-$/au5)
	Compound **3**		
Te(1)−Te(1A)	2.949	0.046	0.073
Ru(1)−Te(1)	2.594	0.108	0.150
Te(1)−Te(2)	2.798	0.056	0.060
Te(2)−Te(3)	2.723	0.060	0.050
	Compound **4**		
Te(3)−Te(4)	3.046	0.041	0.073
Ru(1)−Te(1)	2.638	0.105	0.125
Te(1)−Te(2)	2.716	0.061	0.056
Te(2)−Te(3)	2.740	0.061	0.059

[a] All critical points are (3, −1) bond critical points.[47]

positive curvature of a (3, −1) critical point is along the bond path, where charge density is a minimum at the bond critical point. The formation of a chemical bond is understood as the resultant of two competing effects: the contraction of the charge density toward the interatomic surface and the contraction of the charge density toward each of the interacting nuclei. For selected bond critical points Table 10 shows the charge density (ρ) and the Laplacian of the electron density ($\nabla^2\rho$), with the value of $\nabla^2\rho$ being equal to the sum of the three curvatures of the density at the bond critical point. A plot of ρ values at Te−Te bond critical points versus bond distances (R) reveals an excellent linear correlation, with dρ/dR about −0.033 e$^-$/au.[4] The Laplacian values of $\nabla^2\rho$ increase with bond length in a nonlinear fashion. The ρ values of Te−Te bond critical points are in the range of 0.041 to 0.061 e$^-$/au^3. The $\nabla^2\rho$ values are all positive for Ru−Te and Te−Te bonds, ranging from 0.05 to 0.15 e$^-$/au.[5] Therefore, their interactions are dominated by the attraction of the charge density toward each of the interacting nuclei, characteristic of "closed-shell interactions".[47] Ionic bonds are a typical case of such interactions. Moreover, these critical points for Ru−Te and Te−Te bonds have small ρ values and positive $\nabla^2\rho$ values that are indicative of bonds with ionic character. Nevertheless, in keeping with chemical intuition the Te−Te interactions are manifestly covalent in character, as deduced from the charge distributions.

Acknowledgment. This work was supported in part by the U.S. National Science Foundation under grant CHE-9819385. This work made use of Central Facilities supported by the MRSEC program of the National Science Foundation (DMR00-76097) at the Materials Research Center of Northwestern University.

Supporting Information Available: Crystallographic data in CIF format for [RuCp(PPh$_3$)(μ_2-Se$_2$)]$_2$ (**1**), [Ru$_2$Cp$_2$(μ_3-Se$_2$)(μ_3-Se)]$_2$ (**2**), [(RuCp(PPh$_3$))$_2$(μ_2-(1,4-η:3,6-η)Te$_6$)] (**3**), and [(RuCp(PPh$_3$))$_2$-(μ_2-(1,4-η:3,6-η)Te$_6$)]·CH$_2$Cl$_2$ (**4**). This material is available free of charge via the Internet at http://pubs.acs.org.

IC0483646